EXPERIMENTAL FLOW MEASUREMENT WITH INTEGRAL ORIFICE

Marcelo Filardi, marcelo.filardi@bol.com.br
Smar Equipamento Industriais Ltda. / Rua Dr. Antonio Furlan Junior, 1028 / CEP 14170-480 / Sertãozinho, SP.

Edson Del Rio Vieira, delrio@dem.feis.unesp.br
Sérgio Said Mansur, mansur@dem.feis.unesp.br
UNESP – Ilha Solteira / Av. Brasil Centro, 56 / CEP 15385 000 /Ilha Solteira, SP.

Abstract*. Integral orifice is an industrial flowmeter useful for small diameter lines – typically up to 38 mm – which provides a very precise alignment between the two portions of pipes connected to this device. Experiments have been carried out using PVC pipes with internal diameter of 17 mm in order to check the influence of the tube roughness, the eccentricity of the hole and orifice geometry on the flow measurements. The discharge coefficients have been obtained as a function of the Reynolds number and an empirical correlation has been fitted on experimental points. Results recommend the use of concentric plates with square edge, since they can operate acurately in a wide range of Reynolds number, and its manufacturing process is simpler and cheaper.*

Keywords*: Integral orifice, discharge coefficient, flow measurement, flowmeter.*

NOMENCLATURE

A – Transversal area, m^2
C_V – Velocity-of-approach coefficient
C_d – Discharge coefficient
e – Eccentricity, m
F_g – Geometric factor, m^2
P – Static pressure, Pa
Q – Flowrate, m^3/s
Re – Reynolds number
V – Bulk velocity, m/s
β – Diameters ratio (D_2/D_1)
ΔP – Differential pressure, Pa
ρ – Specific mass, kg/ m^3

1. INTRODUCTION

In spite of the emergence of other flow measurement technologies, differential pressure flowmeters still remain as the first choice for quantify bulk fluid motion of liquid and gases in pipes. In this category of instrument are included the orifice plates, widely employed for monitoring processes in many industrial segments, such as petroleum, chemical, mining, pulp and paper, textile, food processing, and pharmaceutical. Such a device is characterized by its low cost, constructive simplicity, easy installation, and minimal maintenance. From a constructive point of view, it is simply a disc with a circular hole placed in the pipe obstructing the flow. When the fluid reaches the plate, it accelerates to pass through the orifice and a pressure drop proportional to the flowrate is established. By reading the pressure difference across the constriction, the flowrate can be calculated.

Several inaccuracies are associated to the use of orifice plate flowmeters, especially as small diameter lines are employed. In this case, measurements may be significantly affected by tube internal diameter uncertainties and velocity profile distortions due to pipe roughness and/or misalignments, among other factors. The so-called integral orifice flowmeter is designed to mitigate some of these sources of imprecision. Basically, it consists of a self centered orifice plate mounted between two integral blocks having pressure taps. The differential pressure transmitter is directly coupled on these blocks, eliminating the need for fittings, tubing, impulse pipes, valves, adapters, mounting brackets, and welding. Because of this, installation time and cost are reduced. That is mounted directly to the differential pressure transmitter. The integral orifice is commonly used on smaller size lines and is often supplied with a calibrated hole to improve the installed accuracy.

In the present work, experiments using integral orifices have been performed to check the influence of the tube roughness, the eccentricity of the hole, and orifice geometry on the functioning of the instrument. For each case considered, the behavior of the discharge coefficient has been obtained as a function of the Reynolds number.

2. MATHEMATICAL FORMULATION AND TECHNICAL INFORMATION

Pressure difference, ΔP, is measured by means of two pressure taps placed on each side of the orifice plate. According to Bolton (2004), one tap is located in a point equal to the diameter of the pipe upstream of the orifice and the other equal to half diameter downstream. Nevertheless, this information is valid only when radius taps are employed, since each type of tap is positioned at a different location relatively to the plate. Other commonly used taps

include corner taps, flange taps, full flow taps, and contracta taps. Corner taps are preferred with integral orifice assemblies and allow capturing the pressure as close as possible to the faces of the plate.

Whatever the type of pressure tap, the narrowest section of the flow across an orifice plate occurs downstream the orifice and is referred to as the *vena contracta*. In fact, as represented in Fig. 1, after the flow passes through the orifice the flow continues to decrease in cross-sectional area before to expand. The transversal area and location of the *vena contracta* are dependent on the geometry of the orifice plate and the physical properties of the fluid. Moreover, such information is not required for flow measurement because only the diameters of the tube and the hole are needed to obtain the ideal flowrate as a function of the pressure drop across the plate.

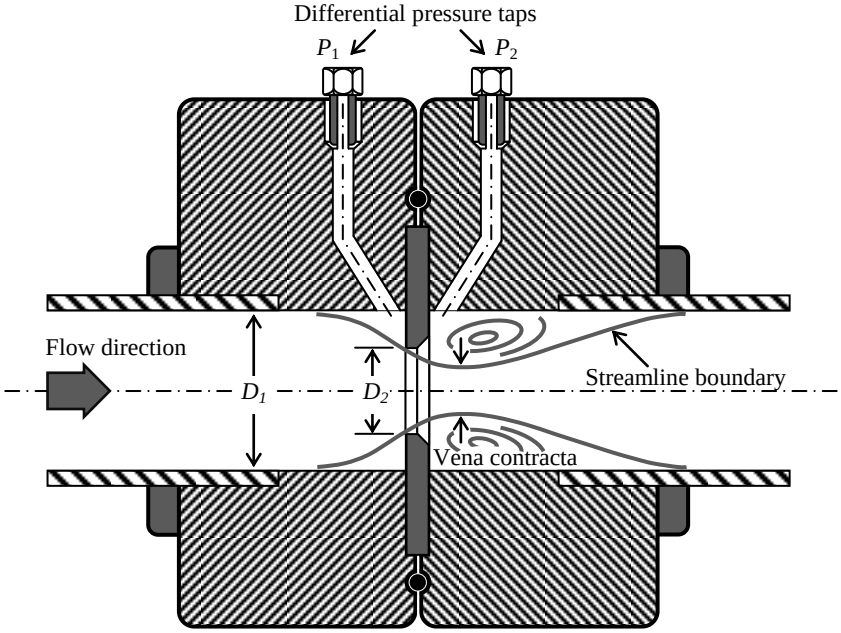

Figure 1: Integral orifice flowmeter.

Derivation of an equation to relate pipe flowrate and pressure drop across an orifice plate is based on Bernoulli and mass conservation principles. For an isothermal, inviscid, and steady-state flow of a constant density fluid these two principles applied along a horizontal streamline between points (1) and (2) may be written respectively as:

$$P_1 + \frac{1}{2}\rho V_1^2 = P_2 + \frac{1}{2}\rho V_2^2 \tag{1}$$

$$A_1 V_1 = A_2 V_2 \tag{2}$$

Considering β as the diameters ratio D_2/D_1 and combining Eqs. (1) and (2), the following relation may be founded to calculate the theoretical flowrate:

$$Q_{ideal} = A_2\ \beta^2 \left(\frac{2\,(P_1 - P_2)}{\rho\,(1-\beta^4)} \right)^{1/2} = A_2\ \beta^2\ \frac{\sqrt{2\,\Delta P/\rho}}{\sqrt{1-\beta^4}} \tag{3}$$

The term $\left(\sqrt{1-\beta^4}\right)^{-1}$ is a geometric constant frequently referred in technical literature as velocity-of-approach coefficient, and denoted by C_V. Thus, Eq. (3) may be rewritten as:

$$Q_{ideal} = C_V\ A_2\ \beta^2 \sqrt{2\,\Delta P/\rho} \tag{4}$$

Nevertheless, the product $C_V\ A_2\ \beta^2 \sqrt{2}$ is also a dimensional geometric constant, F_g, and Eq. (4) may be put in the form:

$$Q_{ideal} = F_g \sqrt{\Delta P/\rho} \tag{5}$$

For real fluid flows, viscosity and turbulence effects convert part of flow kinetic energy into heat. Besides, the flow across orifice plates is quite complex and pressure taps are not installed exactly at the points considered in the mathematical formulation. In order to account frictional effects and other inaccuracy sources, a discharge coefficient, C_d, defined as:

$$C_d \equiv \frac{Q_{actual}}{Q_{ideal}} = \frac{Q_{actual}}{F_g \sqrt{\Delta P / \rho}} \tag{6}$$

is introduced in Eq. (5) to reduce the flowrate Q_{ideal}. For a given orifice plate, the discharge coefficient C_d varies mainly with the Reynolds number and must be experimentally determined by measuring the actual flowrate and the differential pressure through the orifice plate.

3. EXPERIMENTAL APPARATUS AND PROCEDURE

The experimental runs have been carried out using the installation shown in Fig. 2. Its operation is fairly simple and can be described as follows. Tap water (1) is supplied to a cylindrical stagnation chamber (5) equipped with two perforated plates (3) to prevent the propagation of hydrodynamics instabilities until the entrance nozzle (4). A deaeration pipe (2) is connected to the top of the stagnation chamber for removing gas bubbles. A PVC pipe with 17 mm of internal diameter (6) leads the fluid to the flowmeter, formed by an integral orifice device (20) coupled to a differential pressure transmitter (7). An elevated curve (13) was inserted downstream the flowmeter to keep the pipeline always filled with water. A ball valve (16) is used to control the fluid flow. Actual mass flowrate is accurately measured by a standard system formed by a digital balance (18), a reservoir (19), a chronometer (17), and a two-way vane (24).

Pressure drop data through orifice plate are automatically captured by means of a Smar acquisition system. The electrical signal from the differential transmitter (7) is driven to the signal processing system, consisting of a 24 V power supply, a digital controller (11), and a signal conversion module (12). Data are transmitted to a PC (15) by a flexible cable to a RJ45 network connection (14) and recorded by data capture software (15).

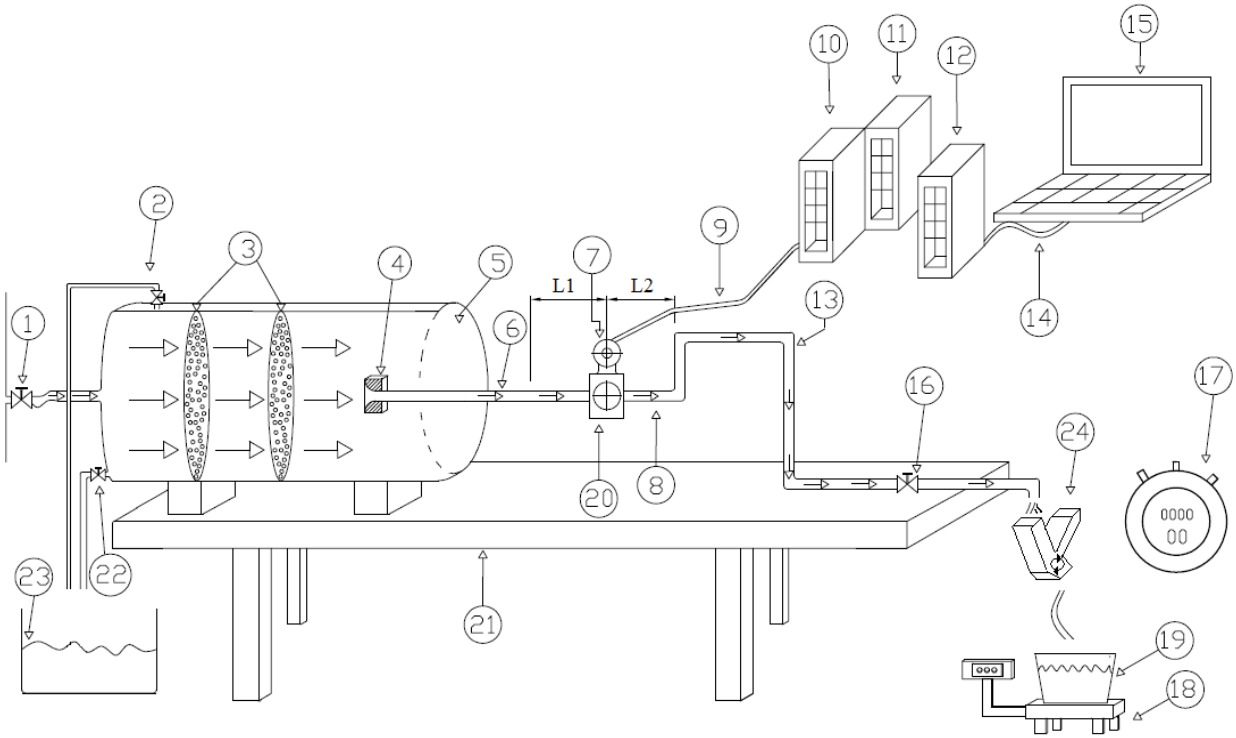

Figure 2. Experimental apparatus and instrumentation.

The orifice plates have been manufactured in strict accordance with the standard ISA RP 3.2. The tests have been performed with different orifice plates, varying the diameters (D_2 = 3.80, 5.01, and 8.59 mm), the eccentricities (e = 0 and $D_2/2$), and the edge shapes of the holes (sharp, conic, and quadrant). Figure 2 shows an exploded view of the integral orifice, as well as this assembly coupled to the pressure transmitter by means of corner taps.

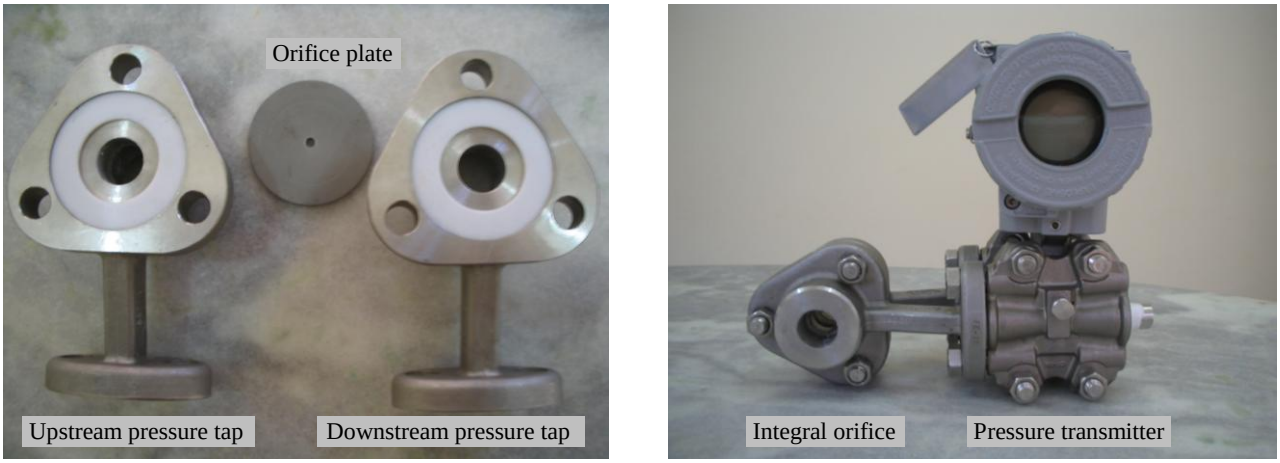

(a) Exploded view. (b) Assembly view.

Figure 2. Integral orifice assembly and pressure transmitter.

Two types of PVC pipes have been used in the tests, both with 20 mm OD and 17 mm ID. The first one is a standard pipe NBR 5648 PN 750 kPa, with an average internal roughness of 0.8 micrometers. In the second pipe, a marked artificial roughness has been produced, by means of a spiral square groove, as illustrated in Fig. 3. The groove is 1 mm wide, 1 mm deep, and has been made with a spiral angle of 5 degrees.

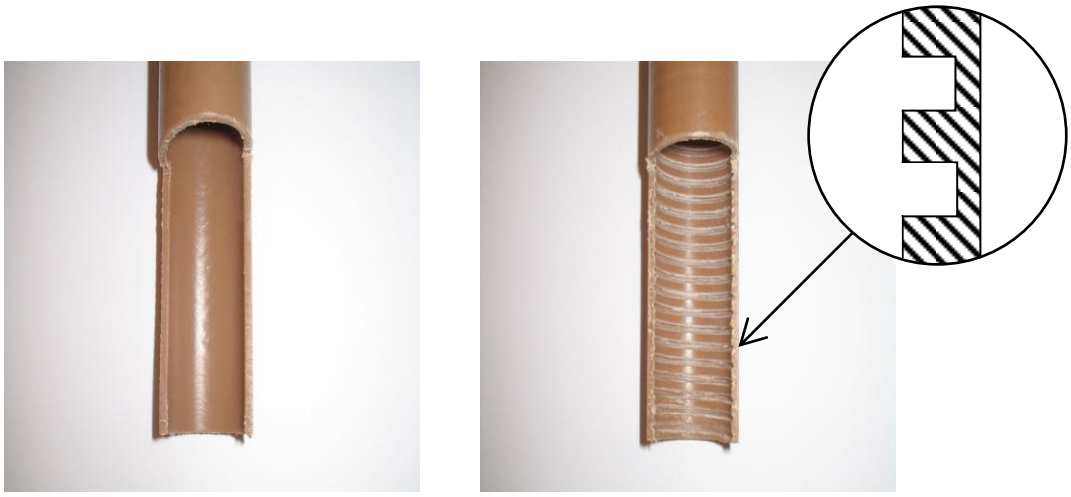

(a) Tube 1: Smooth pipe. (b) Tube 2: Roughness pipe.

Figure 3. Pipe configurations.

4. RESULTS

All the discharges coefficients obtained experimentally are shown in Fig. 4 as a function of the Reynolds number. Experimental uncertainties have been estimated according to Moffat (1988) and are presented in Table 2. For the flow in smooth pipe, Eq. (7) has been fitted from the experimental data to calculate the discharge coefficient for concentric orifices plates with holes with square edge and diameters of 3.80 mm (E001), 5.01 mm (E002), and 8.59 mm (E003). Using parameters *a*, *b*, *c*, and *d* shown in Table 1, Eq. (7) represents experimental values with a maximum deviation less than 1%.

$$C_d = \frac{a + c\,Re^{0.5}}{1 + b\,Re^{0.5} + d\,Re} \tag{7}$$

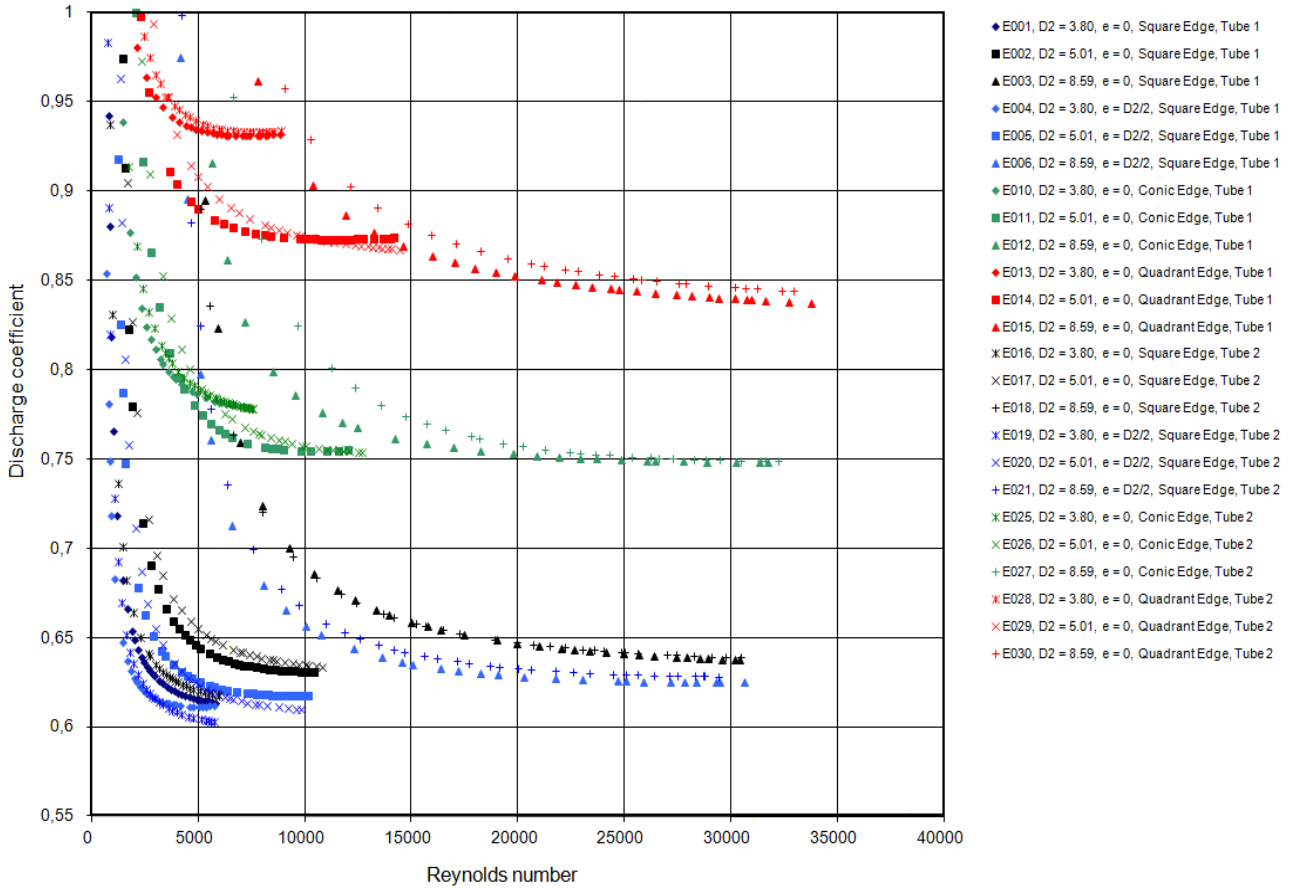

Figure 4. Results of discharge coefficients *versus* Reynolds number.

Table 1. Parameters for Eq. (7).

Test	***a***	***b***	***c***	***d***	***Re* (start)**	***Re* (end)**	R^2
E001	0.501194	– 0.041487	– 0.023034	2.02628E-05	647.6	5803.2	0.997383
E002	0.485645	– 0.031433	– 0.017069	2.07755E-05	1152.2	10453.4	0.998231
E003	0.520524	– 0.016706	– 0.009605	3.37003E-06	3888.9	30184.9	0.985605

Table 2. Relative uncertainty of discharge coefficient C_d.

Reynolds number	**Uncertainty of C_d (%)**		
	D_2 = 3,80 mm (E001)	**D_2 = 5,01 mm (E002)**	**D_2 = 8,59 mm (E003)**
1,000	4.361		
2,000	2.233	2.500	
3,000	1.474	1.495	
4,000	1.195	1.169	2.993
5,000	1.014	0.967	2.209
6,000		0.848	1.715
7,000		0.782	1.314
10,000		0.637	0.803
15,000			0.621
20,000			0.556
25,000			0.524
30,000			0.512

By substituting

$$a = 9.610\,\beta^2 - 7.101\,\beta + 1.649 .$$
$$b = 1.851\,\beta^2 - 1.192\,\beta + 0.112 .$$
$$c = 1.111\,\beta^2 - 0.715\,\beta + 0.067 . \quad \text{and}$$
$$d = 5.251\times10^{-15}\beta^2 - 1.516\times10^{-14}\beta + 2.394\times10^{-15}$$

in Eq. (7), all experimental data obtained for square edge hole and smooth pipe can be represented with a maximum deviation of:

1% for $Re \geq 5.000$ in experiments E001 and E002. and

5% at $Re = 5.000$. decaying continuously until $Re \geq 25.000$. when stabilizes at 1% in experiment E003.

Keeping all other conditions unchanged, difference between results for smooth and roughness pipes are mainly due to turbulence effects. Measurements taken with a hot film anemometer Dantec Streamline 90N10, with a hot-film probe 55R11 adequately positioned upstream the orifice plate have indicated that the presence of grooves on the inner pipe wall substantially modifies the flow conditions in terms of turbulent intensity level, as shown in Fig. 5.

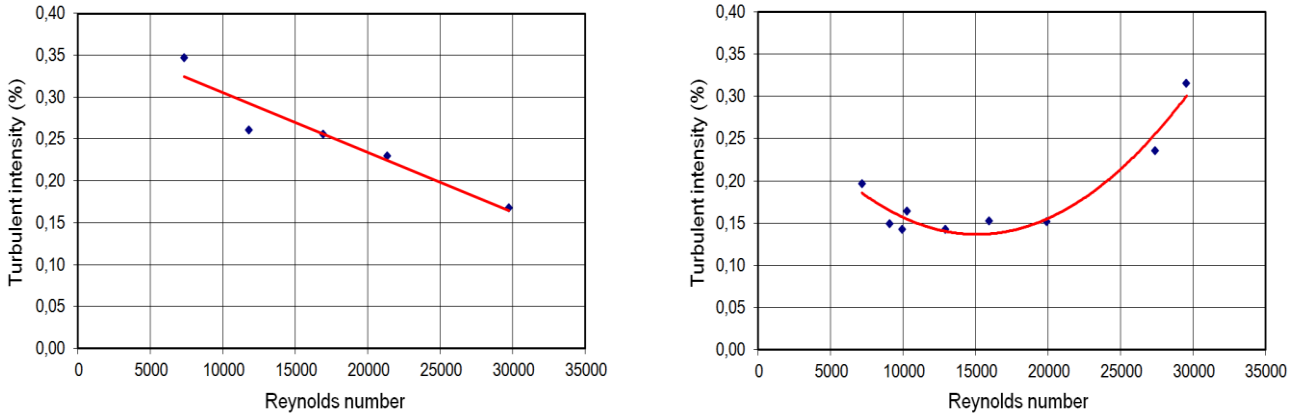

(a) Tube 1: smooth pipe.

(b) Tube 2: rough pipe.

Figure 5. Turbulent intensity of the flow inside pipes *versus* Reynolds number.

6. CONCLUSIONS

Discharge coefficient of orifice plates depends on several factors. The analysis of experimental data has allowed some interesting findings:

- Due to nonlinear dependence between C_d and Re. the accuracy of measurements in the lower portion of the flow range can be strongly degraded. The use of integral orifice plates for Reynolds number less than 5,000 is possible. but its utilization in industrial environment is unusual and not recommended by most standards.
- The minimum recommended Reynolds number for flow through an orifice varies with β and the shape of the edge.
- The shape of the edge considerably affects the coefficient C_d. For $Re \geq 5{,}000$. C_d varies from 0.6 to 0.75 for square edge. from 0.7 to 0.85 for conic edge. and from 0.8 to 1.0 for quadrant edge.
- For very high Reynolds number. the values of C_d trend asymptotically to different limits. depending on the shape of the holes.
- At the same Reynolds number. quadrant edge presented ΔP lower compared to the other edges. The greatest pressure drops are produced by the square edge.
- For the case of square edge. an increase in hole size trends to increase or maintain approximately equal the values of C_d.
- An increase in the eccentricity of the hole tends to decrease or maintain approximately constant the values of C_d. for a fixed Reynolds.
- High pipe roughness modifies turbulence level of the flow and increases the discharge coefficient. especially at low Reynolds number.

7. ACKNOWLEDGEMENTS

The authors are grateful to FUNDUNESP, FAPESP, and SMAR Equipamentos Industriais Ltda. Special thanks to engineers Ivan Carlos Nonato de Souza and Libanio Carlos de Souza for their encouragement.

8. REFERENCES

Bolton. W., Instrumentation and Control Systems. Oxford: Elsevier Ltd.. 2004

Moffat. R.J., Describing the uncertainties in experimental results. Experimental Thermal and Fluid Sciences. v.1. pp.3-16. 1998.

9. RESPONSIBILITY NOTICE

The authors are the only responsible for the printed material included in this paper.